

$^{20}\text{Ne}/^{22}\text{Ne}$ in the Martian Atmosphere: New Evidence from Martian Meteorites. J. Park^{1,2,7}, L. E. Nyquist³, G. F. Herzog², K. Nagao⁴, T. Mikouchi⁵, M. Kusakabe⁶. ¹Kingsborough Comm. Coll., Brooklyn, NY 11235 (Jisun.park@kbcc.cuny.edu), ²Dept. Chem. & Chem. Biol., Rutgers Univ., Piscataway, NJ 08854, ³XI/NASA-JSC, Houston TX 77058 (laurence.e.nyquist@nasa.gov), ⁴Division of Polar Earth-System Sciences, KOPRI (Korea Polar Res. Inst), Incheon 21990, Korea, ⁵Dept. Earth Planet. Sci., Univ. Tokyo, Tokyo 113-0033, Japan, ⁶Dept. Environmental Biol. & Chem., Univ. Toyama, Toyama 930-8555, Japan, ⁷Dept. Earth Planet. Sci., Museum of Natural History (AMNH), New York, NY 10024.

Introduction: Analyses of Ne trapped in “pods” of impact melt in the Elephant Moraine 79001 (EET 79001) Martian meteorite led [1] to suggest ($^{20}\text{Ne}/^{22}\text{Ne}$) ~10 in the Martian atmosphere (MA). In contrast, [2] obtained trapped ($^{20}\text{Ne}/^{22}\text{Ne}$)_{Tr} ~7 from an impact melt vein in Yamato 793605 (Y-793605) and concluded that the isotopic composition of Martian Ne remained poorly defined. A “pyroxene-rich” separate from Dhofar 378 (Dho 378) analyzed by [3] gave a comparatively high trapped Ne concentration and ($^{20}\text{Ne}/^{22}\text{Ne}$) = 7.3±0.2 in agreement with the Y-793605 value. We explore the hypothesis that Martian Ne was trapped in the Dho 378 meteorite in a manner similar to entrapment of terrestrial Ne in tektites [4] strengthening the “Martian atmosphere” interpretation. We also report new data for Northwest Africa 7034 (NWA 7034) that are consistent with the Ne data for Dho 378.

Min-Pet Background for Dho 378 Samples: Plagioclase is mostly recrystallized; a hand-picked sample is called “Light” here. Petrographic observations and EPMA of “pyroxene-rich” portions of a polished thin section of Dho 378 show them to consist of a mixture of dark minerals and Dark, Impact-Melted Material (DIMM). Samples described by [3] as “pyroxene-rich” are called “Dark” here to include both DIMM and black-colored clinopyroxene.

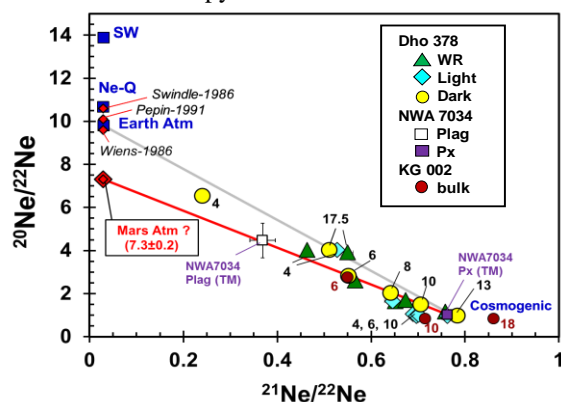


Figure 1. $^{20}\text{Ne}/^{22}\text{Ne}$ vs. $^{21}\text{Ne}/^{22}\text{Ne}$ for NWA 7034 and stepped-temperature extractions of Dho 378. NWA 7034 data are for single heating steps. Step temperatures in 100°C.

Ne isotopic data: Data for Dho 378 [3] are shown in Fig. 1 with new data for NWA 7034 as well as step-heating data for Ksar Ghilane 002 (KG 002) [5]. The NWA 7034 data are for plagioclase and pyroxene

companion samples to those for $^{39}\text{Ar}/^{40}\text{Ar}$ analyses [6]. Ne in NWA 7034 pyroxene (64 μg) is cosmogenic. Ne in NWA 7034 plagioclase has high analytical uncertainty because of the small sample size (22 μg), but plots on a trend line (red) in Fig. 1 through the 600°C, 800°C, and 1000°C extractions of Dho 378 Dark to give ($^{20}\text{Ne}/^{22}\text{Ne}$)_{Tr} = 7.3±0.2 for ($^{21}\text{Ne}/^{22}\text{Ne}$)_{Tr} = 0.029.

Terrestrial Components in Ar, Kr, Xe: Data for 400°C and 1750°C plot above the red ($^{20}\text{Ne}/^{22}\text{Ne}$)_{Tr} trend line (Fig. 1) suggesting the presence of terrestrial Ne. At the lower end of this trend line several analyses show variation in the composition of cosmogenic Ne dependent on whether the phases analyzed were relatively Al-rich (feldspathic) or Al-poor (mafic), or affected by interactions with solar cosmic rays. We have explored these latter possibilities [7], but omit their discussion here. Possible roles of trapped terrestrial noble gases are of greater interest to interpreting ($^{20}\text{Ne}/^{22}\text{Ne}$)_{Tr}, and are revealed by examining isotopic mixing relationships for Ar, Kr, and Xe (Fig. 2).

The compositions of some end member components are shown in Fig. 2. Both EA and EFA derive from terrestrial gas. Previously defined Martian components are not clearly visible in the Dho 378 data, which appear instead to define a new Mars-Interior component here called MI3 to distinguish it from previously defined Chass-S and Chass-E.

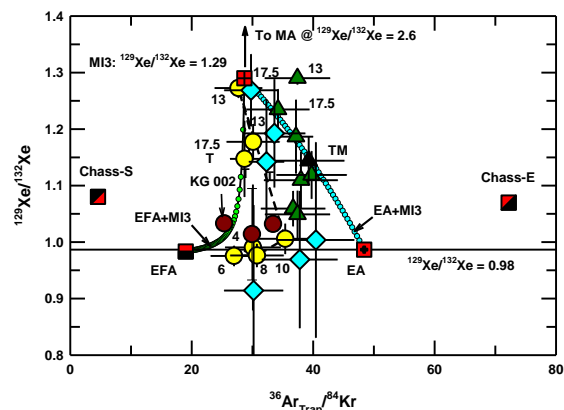


Figure 2. Isotopic mixing relationships among Ar, Kr, and Xe end member components. EA = Earth Air, EFA = Elementally Fractionated Air, MA = Mars Atmosphere, Chass-S and Chass-E = putative martian interior components, MI3 = apparent third Martian Interior component. Symbols for new data as in Figure 1. Step-heating temperatures in 100°C.

Arrhenius Diagrams for Noble Gas Release: Cursory examination of Figs. 1 and 2 seems to lead to contradictory conclusions: Fig. 1 shows that the 600-1000°C extractions of Dho 378 Dark are key to the interpretation that the $(^{20}\text{Ne}/^{22}\text{Ne})_{\text{Tr}}$ trend line represents Martian atmosphere, whereas Fig. 2 suggests that the heavy noble gases in these extractions are a mixture of gases of terrestrial origins. We use Arrhenius diagrams (Fig. 3) to clarify the situation.

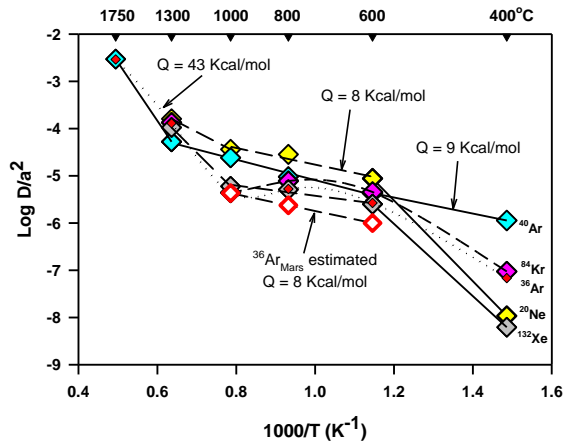


Figure 3. Arrhenius diagrams for the stepped-temperature release of noble gases from Dho 378 Dark. Total ^{36}Ar release is shown by the smaller red diamonds.

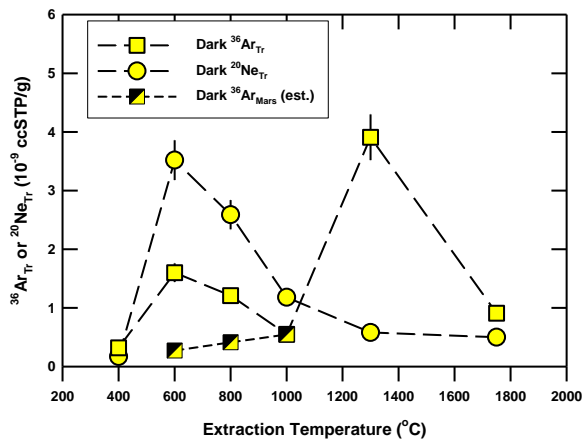


Figure 4. Release of $^{20}\text{Ne}_{\text{Tr}}$ and $^{36}\text{Ar}_{\text{Tr}}$ as a function of extraction temperature for Dho 378 Dark. Data shown as $^{36}\text{Ar}_{\text{Mars}}$ (est.) are corrected for a component of terrestrial ^{36}Ar .

Trapped Ne and Ar Release Profiles: Arrhenius diagrams (Fig. 3), like more conventional gas release diagrams (Fig. 4), show the noble gases to have been released from Dho 378 Dark in two stages following the presumed desorption of the most loosely bound terrestrial components during pre-heat. At the intermediate, 600-1000°C extractions, ^{36}Ar , ^{84}Kr , and ^{132}Xe exhibit Arrhenius profiles characteristic of reservoir exhaustion. For these gases, the rate of release decreases with increasing temperature until a second, higher temperature reservoir begins releasing at ~1000°C.

Fig. 4 shows the release of trapped $(^{20}\text{Ne})_{\text{Tr}}$ after correction for cosmogenic Ne. $(^{20}\text{Ne})_{\text{Tr}}$ decreases steadily from its maximum at $T=600^\circ\text{C}$. The plot for trapped ^{36}Ar (like those for Kr and Xe; not shown) has two peaks. We attribute the high-temperature (T) peak to the release of Martian interior gas from minerals that melt at high T. The low-T plot (400-1000 °C) parallels that for $^{20}\text{Ne}_{\text{Tr}}$. We therefore attribute most but not all of the low-T Ar peak to EFA-Ar that accompanies the low-T EFA-Kr and EFA-Xe. (See Fig. 2).

If we assume equal activation energies (8 kcal/mol; Fig. 3) for $^{36}\text{Ar}_{\text{Tr}}$ and ^{20}Ne and that all of the $^{36}\text{Ar}_{\text{Tr}}$ ($5.46 \times 10^{-10} \text{ cm}^3\text{STP/g}$) at 1000°C is Martian, we obtain $\sum_{T=600}^{1000} ^{36}\text{Ar}_{\text{Tr}}(T) = 1.23 \times 10^{-9} \text{ cm}^3\text{STP/g}$ compared to summed $^{20}\text{Ne}_{\text{Tr}} = 7.29 \times 10^{-9} \text{ cm}^3\text{STP/g}$ over the same temperature range, and an ~30-fold enhancement in $(^{20}\text{Ne}/^{36}\text{Ar})_{\text{Tr}}$ compared to the Martian atmospheric $(^{20}\text{Ne}/^{36}\text{Ar})_{\text{MA}} \sim 0.2$ [7], less than, but similar to the >100-fold enrichments of Ne/Ar in tektites [4]. We attribute Ne enrichment to the influence of the smaller atomic radius of Ne compared to Ar, Kr, and Xe on their respective Henry’s Law constants. (See [8]).

Implications: Our observations reinforce the suggestion that $(^{20}\text{Ne}/^{22}\text{Ne})_{\text{MA}} = 7.3 \pm 0.2$, a value important in modeling the Ne isotopic evolution of the Martian atmosphere. Fig.5 shows that $(^{20}\text{Ne}/^{22}\text{Ne})_{\text{MA}} \sim 7.3$ could evolve from an initial, Mars juvenile $(^{20}\text{Ne}/^{22}\text{Ne})$ like that of Ne-Q, which could explain some prior measurements of “Martian” $^{20}\text{Ne}/^{22}\text{Ne} \sim 10$.

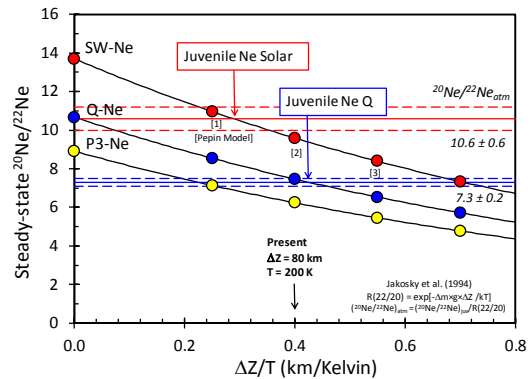


Figure 5. Some possible evolution scenarios for $(^{20}\text{Ne}/^{22}\text{Ne})_{\text{MA}}$ using the model of [9].

References: [1] Pepin R. O. (1991) *Icarus*, 92, 2-79. [2] Garrison D. H. and Bogard D. D. (1998) *MAPS*, 33, 721-736. [3] Park J. and Nagao K. (2006) *LPS XXXVII*, Abstract #1110. [4] Matsubara K. and Matsuda J. (1991) *Meteoritics* 26, 217-220. [5] Llorca J. et al. (2013) *Met. Planet. Sci.*, 48, 493-513. [6] Lindsay F. N. et al. (2016) *47th LPSC*, Abstract #3013. [7] Park J. et al. (2017) in preparation. [8] Lux G. (1987) *GCA*, 51, 1549-1560. [9] Jakosky B. M. et al. (1994) *Icarus*, 111, 271-288.